Wave Propagation in Functionally Graded Piezoelectric-piezomagnetic Rectangular Rings

Yuchun Duan[1], **Xiaoming Zhang**[2,3], **Yuqing Wang**[2] and **Jiangong Yu**[2]

Abstract: The ring ultrasonic transducers are widely used in the ocean engineering and medical fields. This paper proposes a double orthogonal polynomial series approach to solve the wave propagation problem in a functionally graded piezoelectric-piezomagnetic (FGPP) ring with a rectangular cross-section. Through numerical comparison with the available reference results for a pure elastic homogeneous rectangular bar, the validity of the proposed approach is illustrated. The dispersion curves and displacement distributions of various FGPP rectangular bars are calculated to reveal their wave characteristics. The results can be used for the design and optimization of the ring FGPP transducers.

Keywords: wave propagation, rectangular ring, functionally graded material, piezoelectric-piezomagnetic structures, double orthogonal polynomial, dispersion curves.

1   Introduction

With the increasing usage in various applications including sensors, actuators and storage devices piezoelectric-piezomagnetic composites (PPC) have received considerable research effort in the past ten years [Achenbach (2000); Sladek, Sladek, Solek and Atluri (2008); Bishay, Sladek, Sladek and Atluri (2012)]. For the purpose of design and optimization of PPC transducers, wave propagation in various PPC attracted many researchers.

Cao [Cao, Shi and Jin (2012)] investigated Lamb waves propagating in the functionally graded piezoelectric-piezomagnetic material plate by employing the power series technique. Wei [Wei and Su (2006)] studied the axisymmetric flexural wave in PPC cylinders by using 'bar model'. By virtue of propagator matrix and state-

---

[1] Software College, Henan University, KaiFeng, 475001, P.R.China.
[2] School of Mechanical and Power Engineering, Henan Polytechnic University, Jiaozuo 454003, P.R. China.
[3] Corresponding Author. E-mail: zxmworld11@hpu.edu.cn

vector approaches, Chen [Chen, Pan and Chen (2007)] presented an analytical treatment for the propagation of harmonic waves in PPC multilayered plates. Wu [Wu, Yu and He (2008)] used the orthogonal polynomial approach to investigate the wave propagating characteristics in the non-homogeneous magneto-electro-elastic plates. The polynomial approach was also applied to calculate the guided wave in imhomogeneous magneto-electro-elastic cylindrical plates [Yu and Wu (2009)] and spherical plates [Yu and Ma (2010); Xue, Pan and Zhang (2011)] proposed a simple nonlinear model to investigate the solitary waves in a magneto-electro-elastic circular bar based on the the Jacobi elliptic function expansion method. Using a self-adjoint method, the wave propagation in a magneto-electro-elastic square column was studied by Wei [Wei and Su (2008)].

Wave propagation in piezoelectric-piezomagnetic periodically layered structures received attentions [Liu, Wei and Fang (2010); Pang, Wang, Liu and Fang (2010); Zhao, Zhong and Pan (2012)] for analyzing the band gaps The penetration depth of the BleusteinGulyaev waves in a functionally graded transversely isotropic electro-magneto-elastic half-space was discussed by Li [Li Jin and Qian (2013)]. Sun [Sun, Ju, Pan and Li (2011)]and Nie [Nie, Liu, Fang and An (2012)] investigated the effects of the imperfect interface on the SH waves propagating in piezoelectric-piezomagnetic layered structures. The reflection and transmission of plane waves at an imperfectly bonded interface between piezoelectric-piezomagnetic media was discussed by Pang [Pang and Liu (2011)] By using Legendre and Laguerre polynomial approach, Matar [Matar, Gasmi, Zhou, Goueygou and Talbi (2013)] computed propagation constants and mode shapes of elastic waves in layered piezoelectric-piezomagnetic composites. The propagation of SH wave in the layered functionally gradient piezoelectric-piezomagnetic structure was studied by Singh [Singh and Rokne (2013)].

As a common structure, the ring ultrasonic transducer has been widely used in ocean engineering and medical fields. But few investigations on the wave propagation in ring transducers have been reported. This paper proposed a double orthogonal polynomial series approach to solve the wave propagation problem in a functionally graded piezoelectric-piezomagnetic (FGPP) ring with a rectangular cross section. Two material gradient directions (radial direction and axial direction) are respectively considered. The dispersion curves and the displacement profiles of various FGPP rectangular rings are presented and discussed. The investigating results can be used to direct the design and optimization of the ring FGPP transducers. In this paper, traction free and open circuit boundary conditions are assumed.

2   Mathematics and formulation of the problem

Considering an orthotropic ring with a rectangular cross-section in cylindrical co-ordinate $(r\theta, z)$, as shown in Figure.1. h is height in z direction and d is thickness in r direction, and a, b denote the inner and outer radius respectively. The radius to thickness ratio is defined as $\eta = b/(b-a)$ and the width to height ratio is d/h. Its polarization direction is in the r direction.
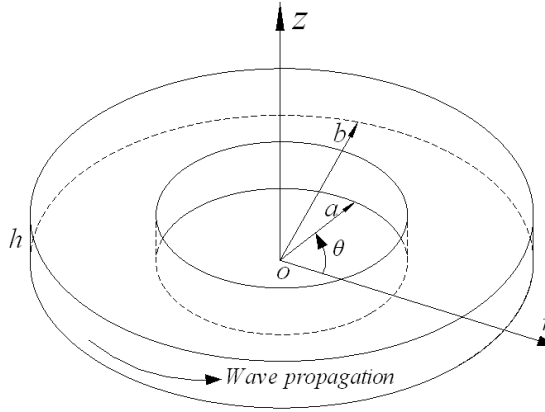

Figure 1: Schematic diagram of a ring with rectangular cross section.

For the wave propagation considered in this paper, the body forces and electric charges and current densities are assumed to be zero. Thus, the dynamic equation for the ring is governed by

$$\frac{\partial T_{rr}}{\partial r} + \frac{1}{r}\frac{\partial T_{r\theta}}{\partial \theta} + \frac{\partial T_{rz}}{\partial z} + \frac{T_{rr} - T_{\theta\theta}}{r} = \rho\frac{\partial^2 u_r}{\partial t^2}$$

$$\frac{\partial T_{r\theta}}{\partial r} + \frac{1}{r}\frac{\partial T_{\theta\theta}}{\partial \theta} + \frac{\partial T_{\theta z}}{\partial z} + \frac{2T_{r\theta}}{r} = \rho\frac{\partial^2 u_\theta}{\partial t^2}$$

$$\frac{\partial T_{rz}}{\partial r} + \frac{1}{r}\frac{\partial T_{\theta z}}{\partial \theta} + \frac{\partial T_{zz}}{\partial z} + \frac{T_{rz}}{r} = \rho\frac{\partial^2 u_z}{\partial t^2} \qquad (1)$$

$$\frac{\partial D_r}{\partial r} + \frac{1}{r}\frac{\partial D_\theta}{\partial \theta} + \frac{\partial D_z}{\partial z} + \frac{D_r}{r} = 0$$

$$\frac{\partial B_r}{\partial r} + \frac{1}{r}\frac{\partial B_\theta}{\partial \theta} + \frac{\partial B_z}{\partial z} + \frac{B_r}{r} = 0$$

where T_{ij}, u_i, D_i and B_i are the stress, elastic displacement, electric displacement and magnetic induction components, respectively and ρ is the density of the material. In this study, quasi-magneto-electro-static assumptioin is made.

The relationships between the general strain and general displacement components can be expressed as

$$\varepsilon_{\theta\theta} = \frac{1}{r}\frac{\partial u_\theta}{\partial \theta} + \frac{u_r}{r}, \quad \varepsilon_{zz} = \frac{\partial u_z}{\partial z}, \quad \varepsilon_{rr} = \frac{\partial u_r}{\partial r}, \quad \varepsilon_{r\theta} = \frac{1}{2}\left(\frac{1}{r}\frac{\partial u_r}{\partial \theta} + \frac{\partial u_\theta}{\partial r} - \frac{u_\theta}{r}\right)$$

$$\varepsilon_{rz} = \frac{1}{2}\left(\frac{\partial u_r}{\partial z} + \frac{\partial u_z}{\partial r}\right), \quad \varepsilon_{\theta z} = \frac{1}{2}\left(\frac{\partial u_\theta}{\partial z} + \frac{\partial u_z}{r\partial \theta}\right), \quad E_\theta = -\frac{1}{r}\frac{\partial \varphi}{\partial \theta}, \quad E_z = -\frac{\partial \varphi}{\partial z},$$

$$E_r = -\frac{\partial \varphi}{\partial r}, \quad B_\theta = -\frac{1}{r}\frac{\partial \psi}{\partial \theta}, \quad B_z = -\frac{\partial \psi}{\partial z}, \quad B_r = -\frac{\partial \psi}{\partial r}.$$

(2)

where ε_{ij}, E_i and H_i are the strain components, the electric field and the magnetic field; ϕ and ψ are the electric potential and the magnetic potential components, respectively.

We introduce the function $I(r,z)$

$$I(r,z) = \pi(r)\pi(z) = \begin{cases} 1, & a \leq r \leq b \quad and \quad 0 \leq z \leq h \\ 0, & elsewhere \end{cases}$$

(3)

where $\pi(r)$ and $\pi(z)$ are rectangular window functions (the subtraction of two Heaviside function), $\pi(r) = \begin{cases} 1, & a \leq r \leq b \\ 0, & elsewhere \end{cases}$ and $\pi(z) = \begin{cases} 1, & 0 \leq z \leq h \\ 0, & elsewhere \end{cases}$. The derivatives along r and z of $I(r,z)$ are delta (r) and delta (z). By introducing the function $I(r,z)$, the traction-free and open-circuit boundary conditions, i.e., $T_{rr} = T_{r\theta} = T_{rz} = T_{\theta z} = T_{zz} = D_r = D_z = H_r = H_z = 0$ at the four boundaries, are automatically incorporated in the constitutive relations of the ring [Datta and Hunsinger (1978)]:

$$T_{\theta\theta} = C_{11}\varepsilon_{\theta\theta} + C_{12}\varepsilon_{zz} + C_{13}\varepsilon_{rr} - e_{31}E_r - q_{31}B_r$$
$$T_{zz} = (C_{12}\varepsilon_{\theta\theta} + C_{22}\varepsilon_{zz} + C_{23}\varepsilon_{rr} - e_{32}E_r - q_{32}B_r)I(r,z)$$
$$T_{rr} = (C_{13}\varepsilon_{\theta\theta} + C_{23}\varepsilon_{zz} + C_{33}\varepsilon_{rr} - e_{33}E_r - q_{33}B_r)I(r,z)$$
$$T_{rz} = (2C_{44}\varepsilon_{rz} - e_{24}E_z - q_{24}B_z)I(r,z)$$
$$T_{r\theta} = (2C_{55}\varepsilon_{r\theta} - e_{15}E_\theta - q_{15}B_\theta)I(r,z)$$
$$T_{\theta z} = 2C_{66}\varepsilon_{\theta z}I(r,z)$$

(4a)

$$D_\theta = 2e_{15}\varepsilon_{r\theta} + \in_{11}E_\theta + g_{11}B_\theta$$
$$D_z = (2e_{24}\varepsilon_{rz} + \in_{22}E_z + g_{22}B_z)I(r,z)$$
$$D_r = (e_{31}\varepsilon_{\theta\theta} + e_{32}\varepsilon_{zz} + e_{33}\varepsilon_{rr} + \in_{33}E_r + g_{33}B_r)I(r,z)$$

(4b)

$$H_\theta = 2q_{15}\varepsilon_{r\theta} + g_{11}E_\theta + \mu_{11}B_\theta$$
$$H_z = (2q_{24}\varepsilon_{rz} + g_{22}E_z + \mu_{22}B_z)\,\mathrm{I}\,(r,z) \tag{4c}$$
$$H_r = (q_{31}\varepsilon_{\theta\theta} + q_{32}\varepsilon_{zz} + q_{33}\varepsilon_{rr} + g_{33}E_r + \mu_{33}B_r)\,\mathrm{I}\,(r,z)$$

where C_{ij}, e_{ij} and q_{ij} are the elastic, piezoelectric, and piezomagnetic coefficients respectively; $\in_{ij}$, g_{ij}, and μ_{ij} are the dielectric, magneto-electric, and magnetic permeability coefficients, respectively.

In this paper, we consider two different material gradient directions, namely, the radial direction and the axial direction. For FGPP rings that material properties vary in radial direction, we denote them by *r*-directional FGPP rings. For rings that t material properties vary in axial direction, we denote them by *a*-directional FGPP rings. For a *r*-directional FGPP ring, the elastic parameter is dependent on *r*, and can be fitted into the polynomial series of the radius

$$C_{ij}(r) = C_{ij}^{(0)} + C_{ij}^{(1)}\left(\frac{r}{d}\right)^1 + C_{ij}^{(2)}\left(\frac{r}{d}\right)^2 + \cdots + C_{ij}^{(L)}\left(\frac{r}{d}\right)^L \tag{5a}$$

With implicit summation over repeated indices, $C_{ij}(r)$ can be written compactly as

$$C_{ij}(r) = C_{ij}^{(l)}\left(\frac{r}{d}\right)^l \quad l = 0,1,2...,L. \tag{5b}$$

And other material parameters can be treated in the same way,

$$e_{ij}(r) = e_{ij}^{(l)}\left(\frac{r}{d}\right)^l, \quad \in_{ij}(r) = \in_{ij}^{(l)}\left(\frac{r}{d}\right)^l, \quad \rho(r) = \rho^{(l)}\left(\frac{r}{d}\right)^l$$
$$q_{ij}(r) = q_{ij}^{(l)}\left(\frac{r}{d}\right)^l, \quad g_{ij}(r) = g_{ij}^{(l)}\left(\frac{r}{d}\right)^l, \quad \mu_{ij}(r) = \mu_{ij}^{(l)}\left(\frac{r}{d}\right)^l, \quad l = 0,1,2...,L \tag{5c}$$

For an *a*-directional FGPP ring, the material parameters are dependent on *z* and can be expressed as

$$C_{ij}(z) = C_{ij}^{(l)}\left(\frac{z}{h}\right)^l, \quad e_{ij}(z) = e_{ij}^{(l)}\left(\frac{z}{h}\right)^l, \quad \in_{ij}(z) = \in_{ij}^{(l)}\left(\frac{z}{h}\right)^l, \quad \rho(z) = \rho^{(l)}\left(\frac{z}{h}\right)^l,$$
$$q_{ij}(z) = q_{ij}^{(l)}\left(\frac{z}{h}\right)^l, \quad g_{ij}(z) = g_{ij}^{(l)}\left(\frac{z}{h}\right)^l, \quad \mu_{ij}(z) = \mu_{ij}^{(l)}\left(\frac{z}{h}\right)^l, \quad l = 0,1,2...,L. \tag{6}$$

For a free harmonic wave propagating in the circumferential direction of a ring, we assume the displacement, electric potential and the magnetic potential components to be of the form

$$u_r(r,\theta,z,t) = \exp(ikb\theta - i\omega t)U(r,z) \tag{7a}$$

$$u_\theta(r,\theta,z,t) = \exp(ikb\theta - i\omega t)V(r,z) \tag{7b}$$

$$u_z(r,\theta,z,t) = \exp(ikb\theta - i\omega t)W(r,z) \tag{7c}$$

$$\varphi(r,\theta,z,t) = \exp(ikb\theta - i\omega t)X(r,z) \tag{7d}$$

$$\psi(r,\theta,z,t) = \exp(ikb\theta - i\omega t)Y(r,z) \tag{7e}$$

where $U(r,z)$, $V(r,z)$ and $W(r,z)$ represent the amplitude of vibration in the r, θ, z directions respectively; $X(r,z)$ and $Y(r,z)$ represent respectively the amplitudes of electric potential and magnetic potential. k is the magnitude of the wave vector in the propagation direction, and ω is the angular frequency.

Substituting Eqs. (2), (3), (4), (5)/(6) and (7) into Eq. (1), the governing differential equations in terms of the displacement, electric potential and magnetic potential components can be obtained. Here, the case of the r-directional FGPP ring is given:

$$
\begin{aligned}
(r/d)^l \Big\{ &\Big[C_{33}^{(l)}\left(r^2 U,_{rr} + (l+1)\,rU,_r\right) - \left(C_{11}^{(l)} + (kb)^2 C_{55}^{(l)} - lC_{13}^{(l)}\right)U \\
&+ ikb\left(C_{13}^{(l)} + C_{55}^{(l)}\right)rV,_r - ikb\left(C_{11}^{(l)} + C_{55}^{(l)} - lC_{13}^{(l)}\right)V + \left(C_{23}^{(l)} + C_{44}^{(l)}\right)r^2 W,_{rz} \\
&+ \left((l+1)C_{23}^{(l)} - C_{12}^{(l)}\right)rW,_z + C_{44}^{(l)} r^2 U,_{zz} \\
&+ e_{33}^{(l)}\left(r^2 X,_{rr} + (l+1)\,rX,_r\right) - e_{31}^{(l)} rX,_r - (kb)^2 e_{15}^{(l)} X + e_{24}^{(l)} r^2 X,_{zz} \\
&+ q_{33}^{(l)}\left(r^2 Y,_{rr} + (l+1)\,rY,_r\right) - q_{31}^{(l)} rY,_r - (kb)^2 q_{15}^{(l)} Y + q_{24}^{(l)} r^2 Y,_{zz} \Big] I(r,z) \\
&+ \Big[C_{33}^{(l)} r^2 U,_r + C_{13}^{(l)} r\left(ikbV + U\right) + C_{23}^{(l)} r^2 W,_z + e_{33}^{(l)} r^2 X,_r + q_{33}^{(l)} r^2 Y,_r \Big] I(r,z),_r \\
&+ \Big[C_{44}^{(l)} r^2 \left(U,_z + W,_r\right) + e_{24}^{(l)} r^2 X,_z + q_{24}^{(l)} r^2 Y,_z \Big] I(r,z),_z \Big\} = -(r/d)^l \rho^{(l)} r^2 \omega^2 U
\end{aligned}
\tag{8a}
$$

$$
\begin{aligned}
(r/d)^l \Big\{ &\Big[C_{55}^{(l)}\left(r^2 V,_{rr} + (l+1)\,rV,_r\right) - \left((l+1)C_{55}^{(l)} + (kb)^2 C_{11}^{(l)}\right)V \\
&+ ikb\left(C_{13}^{(l)} + C_{55}^{(l)}\right)rU,_r + C_{66}^{(l)} r^2 V,_{zz} + ikb\left(C_{11}^{(l)} + (l+1)C_{66}^{(l)}\right)U \\
&+ ikb\left(C_{12}^{(l)} + C_{66}^{(l)}\right)rW,_z + \left(e_{31}^{(l)} + e_{15}^{(l)}\right)rX,_r \\
&+ 2e_{15}^{(l)} X + \left(q_{31}^{(l)} + q_{15}^{(l)}\right)rY,_r + 2q_{15}^{(l)} Y \Big] I(r,z) + C_{66}^{(l)}\left(r^2 V,_z + ikbrW\right)I(r,z),_z \\
&+ \Big[C_{55}^{(l)}\left(r^2 V,_r + rV + ikbrU\right) + e_{15}^{(l)} rX + q_{15}^{(l)} rY \Big] I(r,z),_r \Big\} = -(r/d)^l \rho^{(l)} r^2 \omega^2 V
\end{aligned}
\tag{8b}
$$

$$
\begin{aligned}
(r/d)^l \Big\{ &\Big[C_{44}^{(l)} \left(r^2 W_{,rr} + (l+1)\, r W_{,r} \right) - (kb)^2 C_{66}^{(l)} W + C_{22}^{(l)} r^2 W_{,zz} \\
&+ \left(C_{23}^{(l)} + C_{44}^{(l)} \right) r^2 U_{,rz} + \left(C_{12}^{(l)} + (l+1) C_{44}^{(l)} \right) r U_{,z} \\
&+ ikb \left(C_{12}^{(l)} + C_{66}^{(l)} \right) r V_{,z} + \left(e_{24}^{(l)} + e_{32}^{(l)} \right) r^2 X_{,rz} + (l+1)\, e_{24}^{(l)} r X_{,z} \\
&+ \left(q_{24}^{(l)} + q_{32}^{(l)} \right) r^2 Y_{,rz} + (l+1)\, q_{24}^{(l)} r Y_{,z} \Big] I(r,z) \\
&+ \Big[C_{23}^{(l)} r^2 U_{,r} + C_{12}^{(l)} r \left(ikb V + U \right) + C_{22}^{(l)} r^2 W_{,z} + e_{32}^{(l)} r^2 X_{,r} + q_{32}^{(l)} r^2 Y_{,r} \Big] I(r,z)_{,z} \\
&+ \Big[C_{44}^{(l)} r^2 \left(W_{,r} + U_{,z} \right) + e_{24}^{(l)} r^2 X_{,z} + q_{24}^{(l)} r^2 Y_{,z} \Big] I(r,z)_{,r} \Big\} = - (r/d)^l \rho^{(l)} r^2 \omega^2 V
\end{aligned}
\tag{8c}
$$

$$
\begin{aligned}
(r/d)^l \Big\{ &\Big[e_{33}^{(l)} \left(r^2 U_{,rr} + (l+1)\, r U_{,r} \right) + e_{31}^{(l)} r U_{,r} - (kb)^2 e_{15}^{(l)} U + e_{24}^{(l)} r^2 U_{,zz} \\
&+ l e_{31}^{(l)} \left(U + V \right) - e_{15}^{(l)} V + \left(e_{31}^{(l)} + e_{15}^{(l)} \right) r V_{,r} + \left(e_{24}^{(l)} + e_{32}^{(l)} \right) r^2 W_{,rz} \\
&+ \left(e_{24}^{(l)} + l e_{32}^{(l)} \right) r W_{,z} + (kb)^2 \in_{11}^{(l)} X + (kb)^2 g_{11}^{(l)} Y - \in_{33}^{(l)} \left(r^2 X_{,rr} + (l+1)\, r X_{,r} \right) \\
&- \in_{22}^{(l)} r^2 X_{,zz} - g_{33}^{(l)} \left(r^2 Y_{,rr} + (l+1)\, r Y_{,r} \right) - g_{22}^{(l)} r^2 Y_{,zz} \Big] I(r,z) \\
&+ \Big[e_{33}^{(l)} r^2 U_{,r} + e_{31}^{(l)} r U + e_{31}^{(l)} r V + e_{32}^{(l)} r^2 W_{,z} - \in_{33}^{(l)} r^2 X_{,r} - g_{33}^{(l)} r^2 Y_{,r} \Big] \\
&\times I(r,z)_{,r} + \Big[e_{24}^{(l)} r^2 U_{,z} + e_{24}^{(l)} r^2 W_{,r} - \in_{22}^{(l)} r^2 X_{,z} - g_{22}^{(l)} r^2 Y_{,z} \Big] I(r,z)_{,z} \Big\} = 0
\end{aligned}
\tag{8d}
$$

$$
\begin{aligned}
(r/d)^l \Big\{ &\Big[q_{33}^{(l)} r \left(r U_{,rr} + (l+1)\, U_{,r} \right) + q_{31}^{(l)} r U_{,r} - (kb)^2 q_{15}^{(l)} U + q_{24}^{(l)} r^2 U_{,zz} \\
&+ l q_{31}^{(l)} \left(U + V \right) - q_{15}^{(l)} V + \left(q_{31}^{(l)} + q_{15}^{(l)} \right) r V_{,r} + \left(q_{24}^{(l)} + q_{32}^{(l)} \right) r^2 W_{,rz} \\
&+ \left(q_{24}^{(l)} + l q_{32}^{(l)} \right) r W_{,z} + (kb)^2 g_{11}^{(l)} X + (kb)^2 \mu_{11}^{(l)} Y_{33}^{(l)} \left(r^2 X_{,rr} + (l+1)\, r X_{,r} \right) \\
&- g_{22}^{(l)} r^2 X_{,zz} - \mu_{33}^{(l)} \left(r^2 Y_{,rr} + (l+1)\, r Y_{,r} \right) - \mu_{22}^{(l)} r^2 Y_{,zz} \Big] I(r,z) \\
&+ \Big[q_{33}^{(l)} r^2 U_{,r} + q_{31}^{(l)} r U + q_{31}^{(l)} r V + q_{32}^{(l)} r^2 W_{,z} - g_{33}^{(l)} r^2 X_{,r} - \mu_{33}^{(l)} r^2 Y_{,r} \Big] \\
&\times I(r,z)_{,r} + \Big[q_{24}^{(l)} r^2 U_{,z} + q_{24}^{(l)} r^2 W_{,r} - g_{22}^{(l)} r^2 X_{,z} - \mu_{22}^{(l)} r^2 Y_{,z} \Big] I(r,z)_{,z} \Big\} = 0
\end{aligned}
\tag{8e}
$$

where a subscript comma indicates partial derivative.

To solve the coupled wave equations, $U(r,z)$, $V(r,z)$, $W(r,z)$, $X(r,z)$ and $Y(r,z)$ are expanded into products of two Legendre orthogonal polynomial series as

$$
U(r,z) = \sum_{m,j=0}^{\infty} p_{m,j}^1 Q_m(r) Q_j(z), \quad V(r,z) = \sum_{m,j=0}^{\infty} p_{m,j}^2 Q_m(r) Q_j(z),
$$

$$W(r,z) = \sum_{m,j=0}^{\infty} p_{m,j}^3 Q_m(r) Q_j(z), \quad X(r,z) = \sum_{m,j=0}^{\infty} p_{m,j}^4 Q_m(r) Q_j(z),$$

$$Y(r,z) = \sum_{m,j=0}^{\infty} p_{m,j}^5 Q_m(r) Q_j(z), \tag{9}$$

where $p_{m,j}^i (i = 1, 2, 3, 4, 5)$ is the expansion coefficients and

$$Q_m(r) = \sqrt{\frac{2m+1}{b-a}} P_m \left(\frac{2r-b-a}{b-a} \right), \quad Q_j(z) = \sqrt{\frac{2j+1}{h}} P_j \left(\frac{2z-h}{h} \right) \tag{10}$$

with P_m and P_j being the *m*th and the *j*th Legendre polynomial. Theoretically, *m* and *j* run from 0 to ∞. However, in practice the summation over the polynomials in Eq. (9) can be truncated at some finite values $m = M$ and $j = J$, when the effects of higher order terms become negligible.

Multiplying each equation by $Q_n(r) \cdot Q_p(z) \cdot e^{-j\omega t}$ with *n* and *p* running respectively from zero to *M* and zero to *J*, and integrating over *z* from zero to *h* and *r* from *a* to *b* and taking advantage of the orthonormality of the polynomials $Q_m(r)$ and $Q_j(z)$, Eq. (8) can be reorganized into a form of the system problem:

$$\begin{aligned} &{}^l A_{11}^{n,p,m,j} p_{m,j}^1 + {}^l A_{12}^{n,p,m,j} p_{m,j}^2 + {}^l A_{13}^{n,p,m,j} p_{m,j}^3 + {}^l A_{14}^{n,p,m,j} p_{m,j}^4 + {}^l A_{15}^{n,p,m,j} p_{m,j}^5 \\ &= -\omega^2 \cdot {}^l M_{n,p,m,j} p_{m,j}^1 \end{aligned} \tag{11a}$$

$$\begin{aligned} &{}^l A_{21}^{n,p,m,j} p_{m,j}^1 + {}^l A_{22}^{n,p,m,j} p_{m,j}^2 + {}^l A_{23}^{n,p,m,j} p_{m,j}^3 + {}^l A_{24}^{n,p,m,j} p_{m,j}^4 + {}^l A_{25}^{n,p,m,j} p_{m,j}^5 \\ &= -\omega^2 \cdot {}^l M_{n,p,m,j} p_{m,j}^2 \end{aligned} \tag{11b}$$

$$\begin{aligned} &{}^l A_{31}^{n,p,m,j} p_{m,j}^1 + {}^l A_{32}^{n,p,m,j} p_{m,j}^2 + {}^l A_{33}^{n,p,m,j} p_{m,j}^3 + {}^l A_{34}^{n,p,m,j} p_{m,j}^4 + {}^l A_{35}^{n,p,m,j} p_{m,j}^5 \\ &= -\omega^2 \cdot {}^l M_{n,p,m,j} p_{m,j}^3 \end{aligned} \tag{11c}$$

$${}^l A_{41}^{n,p,m,j} p_{m,j}^1 + {}^l A_{42}^{n,p,m,j} p_{m,j}^2 + {}^l A_{43}^{n,p,m,j} p_{m,j}^3 + {}^l A_{44}^{n,p,m,j} p_{m,j}^4 + {}^l A_{45}^{n,p,m,j} p_{m,j}^5 = 0, \tag{11d}$$

$${}^l A_{51}^{n,p,m,j} p_{m,j}^1 + {}^l A_{52}^{n,p,m,j} p_{m,j}^2 + {}^l A_{53}^{n,p,m,j} p_{m,j}^3 + {}^l A_{54}^{n,p,m,j} p_{m,j}^4 + {}^l A_{55}^{n,p,m,j} p_{m,j}^5 = 0 \tag{11e}$$

where ${}^l A_{\alpha\beta}^{n,p,m,j} (\alpha, \beta = 1, 2, 3, 4, 5)$ and ${}^l M_{n,p,m,j}$ are the elements of the non-symmetric matrices *A* and *M*, which can be obtained by using Eq. (8).

Eq. (11e) can *be* written as:

$$p_{m,j}^5 = - \left({}^l A_{55}^{n,p,m,j} \right)^{-1} \left({}^l A_{51}^{n,p,m,j} p_{m,j}^1 + {}^l A_{52}^{n,p,m,j} p_{m,j}^2 + {}^l A_{53}^{n,p,m,j} p_{m,j}^3 + {}^l A_{54}^{n,p,m,j} p_{m,j}^4 \right) \tag{12}$$

Substituting Eq. (12) into Eq. (11d),

$$p_{m,j}^4 = {}^l IA^{n,p,m,j} \left\{ \left[{}^l A_{41}^{n,p,m,j} - {}^l AA^{n,p,m,j} \cdot {}^l A_{51}^{n,p,m,j} \right] p_{m,j}^1 \right.$$
$$\left. + \left[{}^l A_{42}^{n,p,m,j} - {}^l AA^{n,p,m,j} \cdot {}^l A_{52}^{n,p,m,j} \right] p_{m,j}^2 + \left[{}^l A_{43}^{n,p,m,j} - {}^{ll} AA^{n,p,m,j} \cdot {}^l A_{53}^{n,p,m,j} \right] p_{m,j}^3 \right\}$$

(13)

where ${}^l AA^{n,p,m,j} = {}^l A_{45}^{n,p,m,j} \left({}^l A_{55}^{n,p,m,j} \right)^{-1}$,

and ${}^l IA^{n,p,m,j} = \left[{}^l A_{45}^{n,p,m,j} \left({}^l A_{55}^{n,p,m,j} \right)^{-1} \cdot {}^l A_{54}^{n,p,m,j} - {}^l A_{44}^{n,p,m,j} \right]^{-1}$.

Substituting Eq. (13) into Eq. (12),

$$p_{m,j}^5 = - \left({}^l A_{55}^{n,p,m,j} \right)^{-1} \left\{ {}^l A_{51}^{n,p,m,j} + A_{54}^{n,p,m,j} \cdot {}^l IA^{j,m} \left[\left({}^l A_{41}^{n,p,m,j} - {}^l AA^{n,p,m,j} \cdot {}^l A_{51}^{n,p,m,j} \right) p_{m,j}^1 \right. \right.$$
$$\left. \left. + \left({}^l A_{42}^{n,p,m,j} - {}^l AA^{n,p,m,j} \cdot {}^l A_{52}^{n,p,m,j} \right) p_{m,j}^2 + \left({}^l A_{43}^{n,p,m,j} - {}^l AA^{n,p,m,j} \cdot {}^l A_{53}^{n,p,m,j} \right) p_{m,j}^3 \right] \right\}$$

(14)

Substituting Eq. (13) and (14) into Eq. (11a), (11b) and (11c), gives:

$$\begin{bmatrix} {}^l \bar{A}_{11}^{n,p,m,j} & {}^l \bar{A}_{12}^{n,p,m,j} & {}^l \bar{A}_{13}^{n,p,m,j} \\ {}^l \bar{A}_{21}^{n,p,m,j} & {}^l \bar{A}_{22}^{n,p,m,j} & {}^l \bar{A}_{22}^{n,p,m,j} \\ {}^l \bar{A}_{31}^{n,p,m,j} & {}^l \bar{A}_{32}^{n,p,m,j} & {}^l \bar{A}_{33}^{n,p,m,j} \end{bmatrix} \left\{ \begin{matrix} p_{m,j}^1 \\ p_{m,j}^2 \\ p_{m,j}^3 \end{matrix} \right\} = -\omega^{2\,l} M_{n,p,m,j} \begin{bmatrix} 1 & 0 & 0 \\ 0 & 1 & 0 \\ 0 & 0 & 1 \end{bmatrix} \left\{ \begin{matrix} p_{m,j}^1 \\ p_{m,j}^2 \\ p_{m,j}^3 \end{matrix} \right\}$$

(15)

where ${}^l \bar{A}_{\alpha\beta}^{n,p,m,j} (\alpha, \beta = 1,2)$ and $M_{n,p,m,j}$ are the elements of a non-symmetric matrix. They can be obtained according to Eqs. (11)-(14) and are given in the Appendix.

So, Eq. (15) forms the eigenvalue problem to be solved. The eigenvalue ω^2 gives the angular frequency of the guided wave, and the eigenvectors $p_{m,j}^i (i = 1, 2, 3, 4, 5)$ allow the displacement components to be calculated, and $p_{m,j}^4$, $p_{m,j}^5$ which can be obtained thanks to Eqs. (13) and (14), determine the electric potential and magnetic potential distributions. By using the relation $Vph = \omega/k$, the phase velocity can be obtained.

3   Numerical results and discussions

In order to calculate the effective parameters of the FGPP ring, the Voigt-type model is used in this study. For the *a*-directional FGPP rectangular ring, it can be expressed as

$$C(z) = C_1 V_1(z) + C_2 V_2(z) \tag{16a}$$

for the r-directional FGPP rectangular ring

$$C(r) = C_1 V_1(r) + C_2 V_2(r), \tag{16b}$$

where $V_i(z)/V_i(r)$ and C_i denote the volume fraction of the ith material and the corresponding physical property of the ith material, respectively, and $\sum V_i(z) = 1/\sum V_i(r) = 1$. So, the properties of the FGPP can be expressed as

$$C(z) = C_2 + (C_1 - C_2)V_1(z), \tag{17a}$$

$$C(r) = C_2 + (C_1 - C_2)V_1(r) \tag{17b}$$

According to Eq. (5) and (6), the gradient profile of the material volume fraction can be expressed as a power series expansion. The coefficients of the power series can be determined using the Mathematica function 'Fit'.

Based on the above mathematical formulation, computer programs in terms of the proposed polynomial method have been written using Mathematica to calculate the dispersion curves and the displacement distributions for various FGPP rectangular rings.

3.1   Comparison with the available solution from transfer matrix method

Because no reference results for the guided waves in FGPP or FG rectangular rings can be found in literature, we consider a homogeneous square steel ring with a very large radius to thickness ratio η=1000 to make a comparison with known results of a straight steel square bar from the semi-analytical finite element method [Hayashi, Song and Rose (2003)]. For the steel square bar, C_L =5.85 km/s, C_T =3.23 km/s and $h = d$=5.08mm. Here, C_L and C_T are respectively the longitudinal and the transverse wave velocities. Figure 2 shows the corresponding dispersion curves, where dotted lines are from Hayashi [Hayashi, Song and Rose (2003)] and dashed lines are obtained from the present approach. As can be seen, the results from the polynomial approach agree well with the reference data, which verifies the correctness and the accuracy of the present method.

3.2   Dispersion curves for FGPP rectangular rings

In this section, we take the $Ba_2TiO_3CoFe_2O_4$ FGPP rectangular rings as examples to discuss the wave characteristics. The bottom surface for the a-directional FGPP rectangular ring and the inner surface for the r-directional FGPP rectangular ring are pure Ba_2TiO_3. The material parameters of the two materials with polarization in the thickness direction are given in Table 1.

Firstly, we consider four linely FGPP square rings (d/h=1): (a) a-directional FGPP ring with η=10; (b) r-directional FGPP ring with η=10; (c) a-directional FGPP
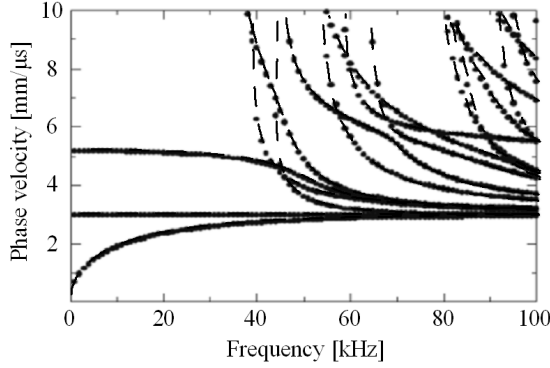
Figure 2: Phase velocity dispersion curves of the square steel rod; dotted lines: Hayashi's results, dashed lines: authors' results.

Table 1: The material properties of the two materials ($C_{ij}(10^9\text{N/m}^2)$, $\in_{ij}$ (10^{-10}F/m^2), e_{ij} (C/m), q_{ij} (N/Am), $\mu_{ij}(10^{-6}\text{Ns}^2/\text{C}^2)$, $\rho(10^3\text{kg/m}^3)$).

Property	C_{11}	C_{12}	C_{13}	C_{22}	C_{23}	C_{33}	C_{44}	C_{55}	C_{66}
Ba$_2$TiO$_3$	166	77	78	166	78	162	43	43	44.6
CoFe$_2$O$_4$	286	173	170.5	286	170.5	269.5	45.3	45.3	56.5
	e_{15}	e_{24}	e_{31}	e_{32}	e_{33}	$\in_{11}$	$\in_{22}$	$\in_{33}$	ρ
Ba$_2$TiO$_3$	11.6	11.6	-4.4	-4.4	18.6	112	112	126	5.8
CoFe$_2$O$_4$	0	0	0	0	0	0.8	0.8	0.93	5.3
	q_{15}	q_{24}	q_{31}	q_{32}	q_{33}	μ_{11}	μ_{22}	μ_{33}	
Ba$_2$TiO$_3$	0	0	0	0	0	5	5	10	
CoFe$_2$O$_4$	550	550	580.3	580.3	699.7	-590	-590	157	

ring with η=2; (d) *r*-directional FGPP ring with η=2. Their phase velocity dispersion curves are shown in Figure 3. It can be seen that the first two wave modes have no cut-off frequencies. This feature is different from that for an infinite FGPP flat plate, in which the first mode has no cut-off frequencies. In a flat plate, only the thickness direction is a finite dimension, but there are two finite dimensions in a rectangular ring. Furthermore, the radius to thickness ratio has a significant effect on the dispersion curves. With the radius to thickness ratio increasing, the difference between the first mode and the second mode of the FGPP square ring becomes small at the low frequency. The reason is that the ring is more and more close to the square bar with the radius to thickness ratio increasing, and for the square bar, the

first two modes is very similar due to the symmetry of the geometry and material distribution. For the FGPP ring with small radius to thickness ratio, the difference between the dispersion curves of the *a*-directional FGPP ring and the ones of the *r*-directional FGPP ring is more significant, which results from two reasons: (1) the piezomagnetic effect and piezoelectric effect are different for the FGPP rings with different polarization directions. (2) For the linely *r*-directional FGPP ring, the volume fraction of the outside material ($CoFe_2O_4$) is higher than that of the inside material (Ba_2TiO_3), and the difference between the two volume fractions become larger with the radius to thickness ratio decreasing, so that the difference of the strength of the piezomagnetic effect and piezoelectric effect is more notable.
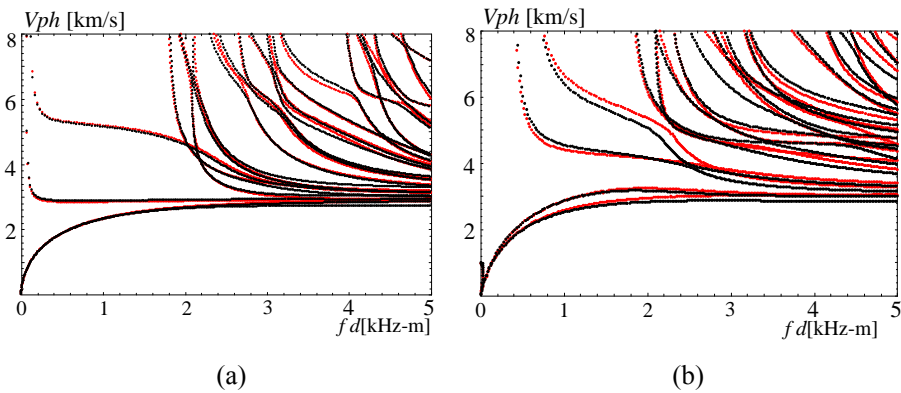

Figure 3: Phase velocity dispersion curves for the FGPP square rings (black lines, a-directional FGPP ring; red lines, r-directional FGPP ring): (a) η=10, (b) η=2.

The cross section of the above four FGPP rings is square. Next, two linely FGPP rectangular rings with η=10 are considered: (e) *r*-directional FGPP ring withd/h=0.5; (f) *a*-directional FGPP ring withd/h=2 Figure 4 shows the corresponding phase velocity dispersion curves. We can see that the width to height ratio can also influence the dispersion curves significantly.

Figure 5 shows the phase velocity dispersion curves for *a*-directional FGPP square rings with different radius to thickness ratios (η=10, η=5, η=3.5, η=2). We can find the effect of the radius to thickness ratio on the dispersion curves is very significant, and the phase velocity decreases with the radius to thickness ratio increasing.

Then, we consider three kinds of different gradient variations, $V_1(r) = \left(\frac{r-a}{h}\right)^t, t =$ 1,2,3, namely, linearly gradient variation, squarely gradient variation and cubically gradient variation. Figure 6 shows the phase velocity dispersion curves of the first four order modes for a-directional FGPP square rings (η=10) with different

(a)   (b)
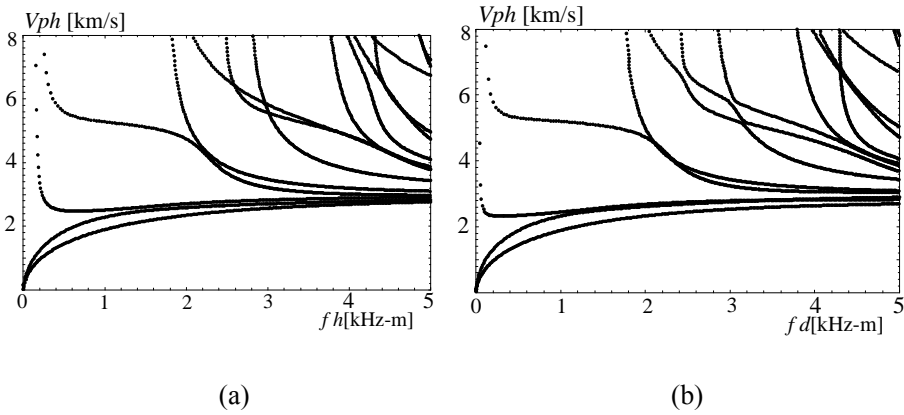
Figure 4: Phase velocity dispersion curves for FGPP rectangular rings: (a) *r*-directional FGPP ring with *d*/*h*=0.5, (b) *a*-directional FGPP ring with *d*/*h*=2.
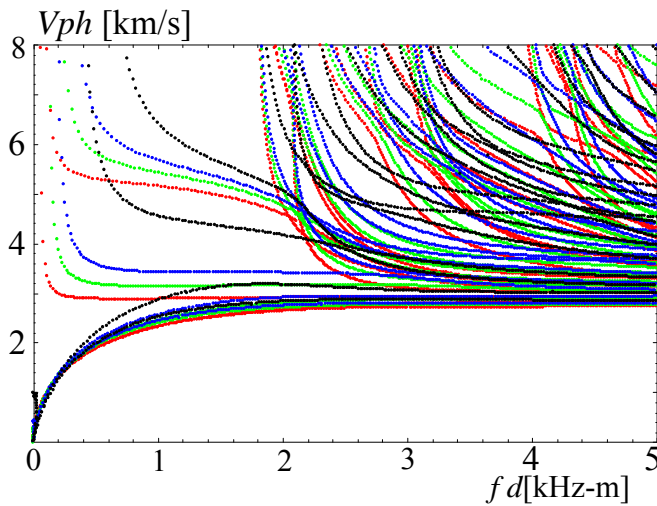


Figure 5: Phase velocity dispersion curves for *a*-directional FGPP square rings with different radius to thickness ratios: red lines, η=10; green lines, η=5; blue lines, η=3.5; black lines, η=2.

gradient variations. The results indicate that the FGPP rings with different gradient variations have different dispersion characteristics. The reason for this is that different gradient variation results in the different material volume fraction. The phase velocity decreases with the power exponent (t) increasing. This is due to the factor that the volume fraction of Ba_2TiO_3 increases with the power exponent (t) increasing, and the body wave speed of Ba_2TiO_3 is lower than that of $CoFe_2O_4$.


(a)   (b)
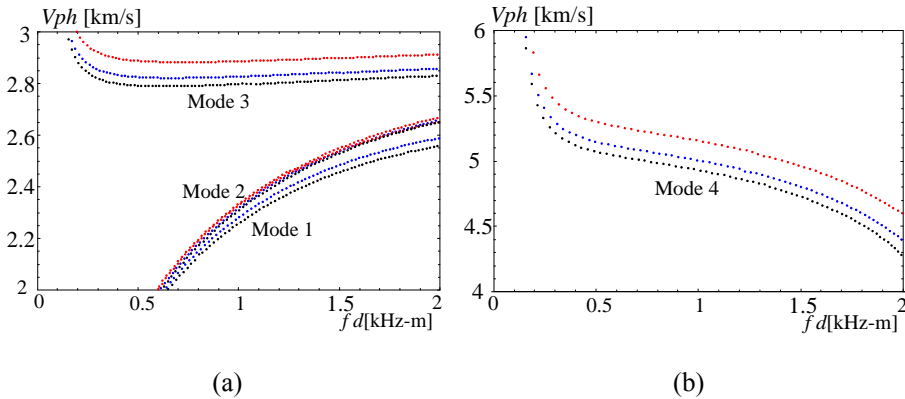
Figure 6: Phase velocity dispersion curves for *a*-directional FGPP square rings with different gradient variations with $\eta=10$ (red lines, linearly gradient variation; blue lines, squarely gradient variation; black lines, cubically gradient variation): (a) mode 1-3; (b) mode 4.

The above three gradient fields are monotonic. Next, a cosinusoidally FGPP ring and a sinusoidally FGPP ring with $\eta=10$ and $d/h=1$ are considered. The corresponding phase velocity dispersion curves are given in Figure 7. We can see that the dispersion characteristics are different for the two FGPP square rings with different gradient fields.

3.3 Displacement shapes

In this section, we discuss the wave characteristics through the mechanical displacement profiles. Figures. 8 and 9 illustrate the displacement shapes of the second and fifth modes for a linearly*a*-directional FGPP square ring at $kd=180$. We can see that most displacements distribute near the bottom edge, namely, the side with more Ba_2TiO_3. The reason lies in that the body wave speed of Ba_2TiO_3 is lower than that of $CoFe_2O_4$. Figures. 10 and 11 show the case for a cosinusoidally *a*-directional FGPP square ring. We can see that that the displacement mostly distribute around the bottom and top sides. That means they mostly distribute around
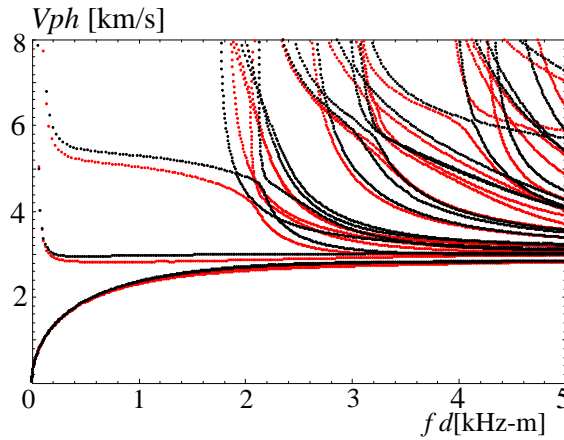
Figure 7: Phase velocity dispersion curves for *a*-directional FGPP square rings with different gradient variations with $\eta=10$ (red lines, cosinusoidally gradient variation; black lines, sinusoidally gradient variation).
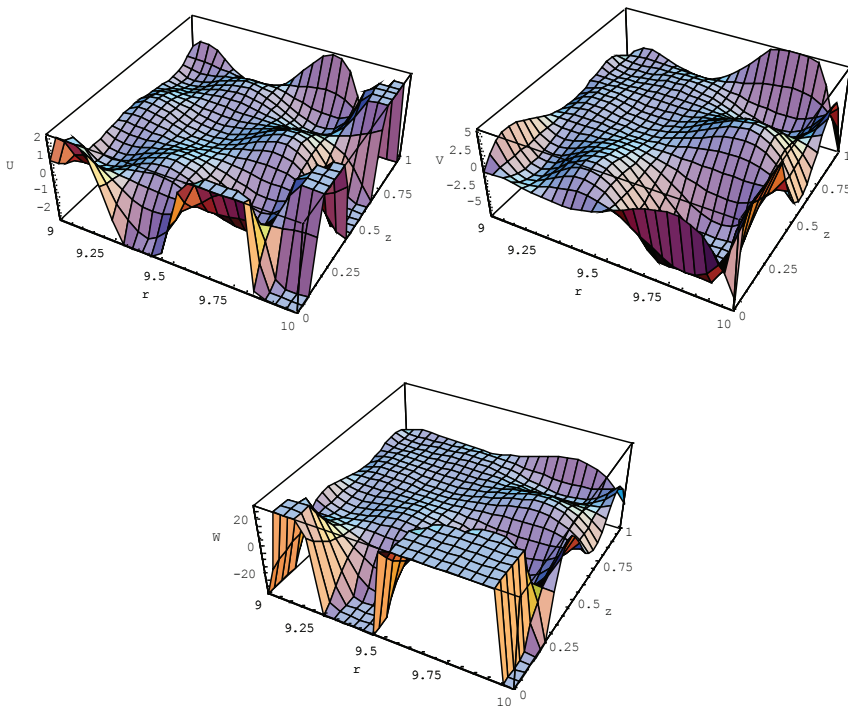
Figure 8: Displacement profiles of the second mode for the linearly *a*-directional FGPP square ring at *kd*=180.
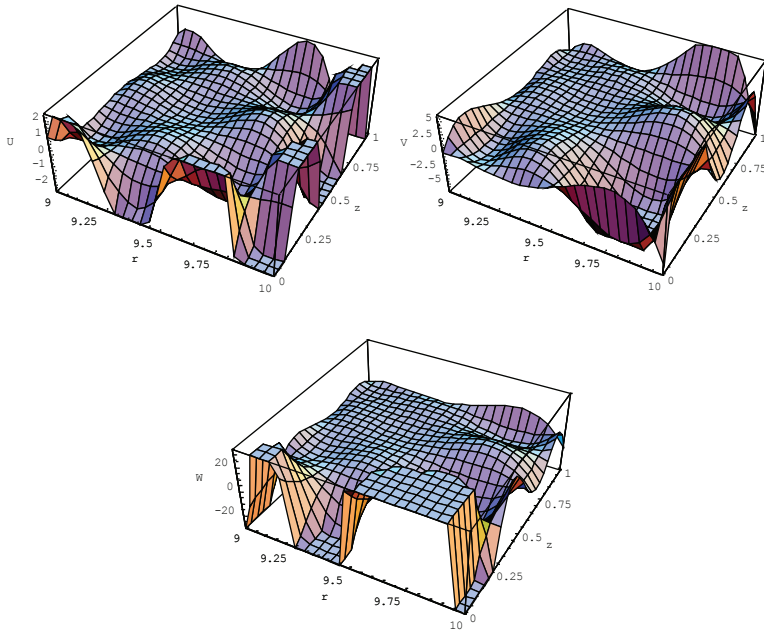
Figure 9: Displacement profiles of the fifth mode for the linearly *a*-directional FGPP square ring at *kd*=180.
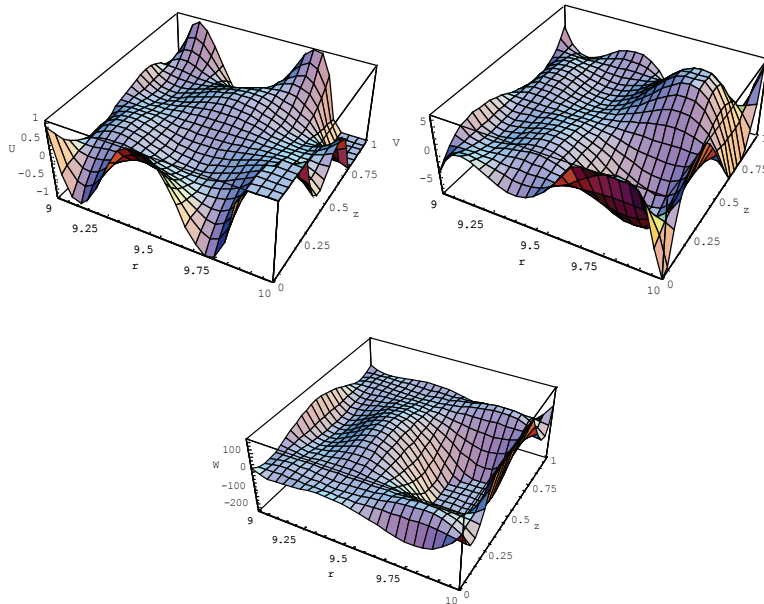
Figure 10: Displacement profiles of the second mode for the cosinusoidally *a*-directional FGPP square ring at *kd*=180.
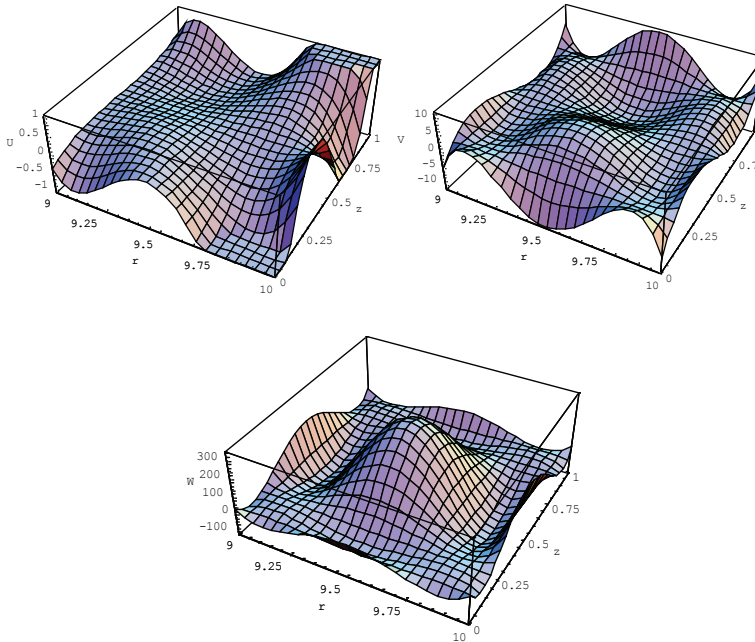
Figure 11: Displacement profiles of the fifth mode for the cosinusoidally-*a*-directional FGPP square ring at *kd*=180.

z=0 and z=1, where the volume fraction of Ba_2TiO_3 is higher. This phenomenon shows the high frequency wave always propagate on the side with more materials of high wave speed. So, through changing the gradient variation of the FGPP ring, we can to obtain any field distributions that we want. Furthermore, in figures 10 and 11, the displacement *w* is symmetric and displacement *u* and *v* are antisymmetric with respect to the *z*-axis, which results from the material volume fraction are symmetrically distributed on the *z*-axis.

4 Conclusions

In this paper, wave propagation analysis of a 2-D FGPP rectangular ring is solved by a double orthogonal polynomial series approach. The dispersion curves and displacement distributions of various FGPP rectangular rings are presented and discussed. According to the numerical results, we can draw the following conclusions:

(a) Numerical comparison of the dispersion curves with reference solutions shows that the double orthogonal polynomial method is appropriate to solve the guided wave propagation problem in 2-D FGPP structures.

(b) The radius to thickness ratio and the width to height ratio and the gradient field all have significant influences on the guided wave charateristics.

(c) High frequency waves propagate predominantly around the side with more material having lower wave speed.

So, through changing the radius to thickness ratio, the width to height ratio and the gradient variation of the FGPP ring, we can obtain the ring transducers with the dispersion features and field distributions that we want.

References

Achenbach, J. D. (2000): Quantitative nondestructive evaluation. *International Journal of Solids and Structures*, vol. 37, pp. 1327.

Bishay, P. L.; Sladek, J.; Sladek, V.; Atluri, S. N. (2012): Analysis of Functionally Graded Magneto-Electro-Elastic Composites Using Hybrid/Mixed Finite Elements and Node-Wise Material Properties. *CmcComputers Materials & Continua*, vol. 29, no. 3, pp. 213261

Cao, X. S.; Shi, J. P.; Jin, F. (2012): Lamb wave propagation in the functionally graded piezoelectric-piezomagnetic material plate. *Acta Mechanica*, vol. 233, no. 5, pp. 10811091

Chen, J. Y.; Pan, E.; Chen, H. L. (2007): Wave propagation in magneto-electro-elastic multilayered plates. *International Journal of Solids and Structures*, vol. 44, pp. 10731085.

Datta, S.; Hunsinger, B. J. (1978): Analysis of surface waves using orthogonal functions. *J. Appl. Phys,* vol. 9, no. 2, pp. 75479.

Hayashi, T.; Song, W. J.; Rose, J. L. (2003): Guided wave dispersion curves for a bar with an arbitrary cross-section, a rod and rail example. *Ultrasonics*, vol. 41, no. 3, pp. 175-183.

Li, P.; Jin, F.; Qian, Z. (2013): Propagation of the BleusteinGulyaev waves in a functionally graded transversely isotropic electro-magneto-elastic half-space. *European Journal of Mechanics-A/Solids*, vol. 37, pp. 1723.

Liu, J.; Wei, W.; Fang, D.(2010): Propagation behaviors of shear horizontal waves

in piezoelectric-piezomagnetic periodically layered structures. *Acta Mechanica Solida Sinica*, vol. 23, no. 1, pp. 77-84.

Matar, O. B.; Gasmi, N.; Zhou, H.; Goueygou, M.; Talbi, A. (2013): Legendre and Laguerre polynomial approach for modeling of wave propagation in layered magneto-electro-elastic media. *The Journal of the Acoustical Society of America*, vol. 133, no. 3, pp. 14151424.

Nie, G. Q.; Liu, J. X.; Fang, X. Q.; An, Z. J. (2012): Shear horizontal (SH) waves propagating in piezoelectricpiezomagnetic bilayer system with an imperfect interface. *Acta Mechanica*, vol. 223, no. 9, pp. 19992009.

Pang, Y.; Liu J. X. (2011): Reflection and transmission of plane waves at an imperfectly bonded interface between piezoelectric and piezomagnetic media. *European Journal of Mechanics-A/Solids*, vol. 30,no. 5, pp. 31740.

Pang, Y.; Wang, Y. S.; Liu, J. X.; Fang, D. N. (2010): A study of the band structures of elastic wave propagating in piezoelectric/piezomagnetic layered periodic structures. *Smart Materials and Structures*, vol. 19, no. 5, pp. 055012.

Singh, B. M.; Rokne, J. (2013): Propagation of SH waves in layered functionally gradient piezoelectric-piezomagnetic structures. *Philosophical Magazine*, vol. 93, no. 14, pp. 16901700.

Sladek, J.; Sladek, V.; Solek, P.; Atluri, S. N. (2008): Modeling of intelligent material systems by the MLPG. *CmesComputer Modeling in Engineering & Sciences*, vol. 34, no. 3, pp. 273-300.

Sun, W. H.; Ju, G. L.; Pan, J. W.; Li Y. D. (2011): Effects of the imperfect interface and piezoelectric/piezomagnetic stiffening on the SH wave in a multiferroic composite. *Ultrasonics*, vol. 51, no. 7, pp. 831838.

Wei, J.; Su, X. Y. (2006): Wave Propagation and Energy Transportation along Cylindrical Piezoelectric Piezomagnetic Material. *Acta Scientiarum Naturalium Universitatis Pekinensis*, vol. 42, pp. 310314

Wei J. P.; Su X. Y. (2008): Steady-state Response of the Wave Propagation in a Magneto-Electro-Elastic Square Column. *CmesComputer Modeling in Engineering & Sciences*, vol. 37, no. 1, pp. 65-84

Wu, B.; Yu, J. G.; He, C. F. (2008): Wave propagation in non-homogeneous magneto-electro-elastic plates. *Journal of sound and vibration*, vol. 317, pp. 250-264.

Xue, C. X.; Pan E.; Zhang S. Y. (2011): Solitary waves in a magneto-electro-elastic circular bar. *Smart Materials and Structures*, vol. 20, no. 10, pp. 105010.

Yu, J. G.; Wu, B. (2009): Circumferential wave in magneto-electro-elastic functionally graded cylindrical curved plates. *European Journal of Mechanics A/Solids*,

vol. 28, no. 3, pp. 560-568

Yu, J. G.; Ma Q. J. (2010): Wave characteristics in magneto-electro-elastic functionally graded spherical curved plates.   *Mechanics of Advanced Materials and Structures*, vol. 17 no. 4, pp. 287 - 301.

Zhao, J.; Zhong, Z.; Pan, Y. (2012): Theoretical study of SH-wave propagation in piezoelectric/piezomagnetic layered periodic structures. *The Journal of the Acoustical Society of America*, vol. 131, no. 4, pp. 3327-3327.

Appendix

The elements of the matrices in Eq. (15) are given by

$$
{}^{l}\bar{A}_{11}^{n,p,m,j} = {}^{l}A_{11}^{n,p,m,j} - {}^{l}A_{15}^{n,p,m,j}\left({}^{l}A_{55}^{n,p,m,j}\right)^{-1}\cdot{}^{l}A_{51}^{n,p,m,j}+
$$
$$
\left({}^{l}A_{14}^{n,p,m,j} - {}^{l}A_{15}^{n,p,m,j}\left({}^{l}A_{55}^{n,p,m,j}\right)^{-1}\cdot{}^{l}A_{54}^{n,p,m,j}\right)\cdot{}^{l}IA^{n,p,m,j}\left({}^{l}A_{41}^{n,p,m,j} - {}^{l}AA^{n,p,m,j}\cdot{}^{l}A_{51}^{n,p,m,j}\right)
$$

$$
{}^{l}\bar{A}_{12}^{n,p,m,j} = {}^{l}A_{12}^{n,p,m,j} - {}^{l}A_{15}^{n,p,m,j}\left({}^{l}A_{55}^{n,p,m,j}\right)^{-1}\cdot{}^{l}A_{52}^{n,p,m,j}+
$$
$$
\left({}^{l}A_{14}^{n,p,m,j} - {}^{l}A_{15}^{n,p,m,j}\left({}^{l}A_{55}^{n,p,m,j}\right)^{-1}\cdot{}^{l}A_{54}^{n,p,m,j}\right)\cdot{}^{l}IA^{n,p,m,j}\left({}^{l}A_{42}^{n,p,m,j} - {}^{l}AA^{n,p,m,j}\cdot{}^{l}A_{52}^{n,p,m,j}\right)
$$

$$
{}^{l}\bar{A}_{13}^{n,p,m,j} = {}^{l}A_{13}^{n,p,m,j} - {}^{l}A_{15}^{n,p,m,j}\left({}^{l}A_{55}^{n,p,m,j}\right)^{-1}\cdot{}^{l}A_{53}^{n,p,m,j}+
$$
$$
\left({}^{l}A_{14}^{n,p,m,j} - {}^{l}A_{15}^{n,p,m,j}\left({}^{l}A_{55}^{n,p,m,j}\right)^{-1}\cdot{}^{l}A_{54}^{n,p,m,j}\right)\cdot{}^{l}IA^{n,p,m,j}\left({}^{l}A_{43}^{n,p,m,j} - {}^{l}AA^{n,p,m,j}\cdot{}^{l}A_{53}^{n,p,m,j}\right)
$$

$$
{}^{l}\bar{A}_{21}^{n,p,m,j} = {}^{l}A_{21}^{n,p,m,j} - {}^{l}A_{25}^{n,p,m,j}\left({}^{l}A_{55}^{n,p,m,j}\right)^{-1}\cdot{}^{l}A_{51}^{n,p,m,j}+
$$
$$
\left({}^{l}A_{24}^{n,p,m,j} - {}^{l}A_{25}^{n,p,m,j}\left({}^{l}A_{55}^{n,p,m,j}\right)^{-1}\cdot{}^{l}A_{54}^{n,p,m,j}\right)\cdot{}^{l}IA^{n,p,m,j}\left({}^{l}A_{41}^{n,p,m,j} - {}^{l}AA^{n,p,m,j}\cdot{}^{l}A_{51}^{n,p,m,j}\right)
$$

$$
{}^{l}\bar{A}_{22}^{n,p,m,j} = {}^{l}A_{22}^{n,p,m,j} - {}^{l}A_{25}^{n,p,m,j}\left({}^{l}A_{55}^{n,p,m,j}\right)^{-1}\cdot{}^{l}A_{52}^{n,p,m,j}+
$$
$$
\left({}^{l}A_{24}^{n,p,m,j} - {}^{l}A_{25}^{n,p,m,j}\left({}^{l}A_{55}^{n,p,m,j}\right)^{-1}\cdot{}^{l}A_{54}^{n,p,m,j}\right)\cdot{}^{l}IA^{n,p,m,j}\left({}^{l}A_{42}^{n,p,m,j} - {}^{l}AA^{n,p,m,j}\cdot{}^{l}A_{52}^{n,p,m,j}\right)
$$

$$
{}^{l}\bar{A}_{23}^{n,p,m,j} = {}^{l}A_{23}^{n,p,m,j} - {}^{l}A_{25}^{n,p,m,j}\left({}^{l}A_{55}^{n,p,m,j}\right)^{-1}\cdot{}^{l}A_{53}^{n,p,m,j}+
$$
$$
\left({}^{l}A_{24}^{n,p,m,j} - {}^{l}A_{25}^{n,p,m,j}\left({}^{l}A_{55}^{n,p,m,j}\right)^{-1}\cdot{}^{l}A_{54}^{n,p,m,j}\right)\cdot{}^{l}IA^{n,p,m,j}\left({}^{l}A_{43}^{n,p,m,j} - {}^{l}AA^{n,p,m,j}\cdot{}^{l}A_{53}^{n,p,m,j}\right)
$$

$$
{}^{l}\bar{A}_{31}^{n,p,m,j} = {}^{l}A_{31}^{n,p,m,j} - {}^{l}A_{35}^{n,p,m,j}\left({}^{l}A_{55}^{n,p,m,j}\right)^{-1}\cdot{}^{l}A_{51}^{n,p,m,j}+
$$
$$
\left({}^{l}A_{34}^{n,p,m,j} - {}^{l}A_{35}^{n,p,m,j}\left({}^{l}A_{55}^{n,p,m,j}\right)^{-1}\cdot{}^{l}A_{54}^{n,p,m,j}\right)\cdot{}^{l}IA^{n,p,m,j}\left({}^{l}A_{41}^{n,p,m,j} - {}^{l}AA^{n,p,m,j}\cdot{}^{l}A_{51}^{n,p,m,j}\right)
$$

$$
{}^{l}\bar{A}_{32}^{n,p,m,j} = {}^{l}A_{32}^{n,p,m,j} - {}^{l}A_{35}^{n,p,m,j}\left({}^{l}A_{55}^{n,p,m,j}\right)^{-1}\cdot{}^{l}A_{52}^{n,p,m,j}+
$$
$$
\left({}^{l}A_{34}^{n,p,m,j} - {}^{l}A_{35}^{n,p,m,j}\left({}^{l}A_{55}^{n,p,m,j}\right)^{-1}\cdot{}^{l}A_{54}^{n,p,m,j}\right)\cdot{}^{l}IA^{n,p,m,j}\left({}^{l}A_{42}^{n,p,m,j} - {}^{l}AA^{n,p,m,j}\cdot{}^{l}A_{52}^{n,p,m,j}\right)
$$

$$
{}^{l}\bar{A}_{33}^{n,p,m,j} = {}^{l}A_{33}^{n,p,m,j} - {}^{l}A_{35}^{n,p,m,j}\left({}^{l}A_{55}^{n,p,m,j}\right)^{-1}\cdot{}^{l}A_{53}^{n,p,m,j} +
$$

$$
\left({}^{l}A_{34}^{n,p,m,j} - {}^{l}A_{35}^{n,p,m,j}\left({}^{l}A_{55}^{n,p,m,j}\right)^{-1}\cdot{}^{l}A_{54}^{n,p,m,j}\right)\cdot{}^{l}IA^{n,p,m,j}\left({}^{l}A_{43}^{n,p,m,j} - {}^{l}AA^{n,p,m,j}\cdot{}^{l}A_{53}^{n,p,m,j}\right)
$$